Journal of Magnetic Resonance **142,** 254–265 (2000)
doi:10.1006/jmre.1999.1919, available online at http://www.idealibrary.com on IDEAL®

Fast and Accurate Characterization of Biological Membranes by EPR Spectral Simulations of Nitroxides

J. Štrancar,[1] M. Šentjurc, and M. Schara

J. Stefan Institute, Jamova 39, 1000 Ljubljana, Slovenia

Received April 12, 1999; revised July 29, 1999

A method by which it is possible to characterize the membranes of biological samples on the basis of the EPR spectral lineshape simulation of membrane-dissolved nitroxide spin probes is described. The presented simulation procedure allows the determination of the heterogeneous structure of biological membranes and fluidity characteristics of individual membrane domains. The method can deal with isotropic and anisotropic orientations of nitroxides introduced into the biological samples described by restricted fast motion with a correlation time between 0.01 and 10 ns. The linewidths of the Lorentzian lineshapes are calculated in a restricted fast-motion approximation. In the special case of samples with high concentrations of nitroxides or in the presence of paramagnetic ions, the lineshapes are calculated directly from the exchange-coupled Bloch equations. The parameters describing ordering, relaxation, polarity, and the portions of the individual spectral components are extracted by optimizing the simulated spectra to the experimental spectrum with either a Simplex or a Monte Carlo algorithm. To improve the algorithm's efficiency, a new way of characterizing the goodness of fits is introduced. The new criterion is based on the standard least-squares function, but with special weighting of the partial sums. Its benefits are confirmed with membrane spectral simulation. Two classes of examples—simulation and optimizations of synthetic spectra to evaluate the accuracy of the optimization algorithms and simulation and optimization of EPR spectra of nitroxides in liposome suspensions in the presence of a broadening agent and in human leukocytes are shown.

Key Words: **membranes; nitroxides; EPR; simulations; spin exchange.**

INTRODUCTION

Biological membranes have been investigated by various techniques allowing the evaluation of different membrane characteristics. Electron paramagnetic resonance (EPR) spectroscopy based on labeling with nitroxide spin probes (SP) has proven to be a powerful method for studying biological membranes (*1*, *2*). It can detect alterations induced by biologically active substances or the involvement of pathological conditions (*3–5*). The recorded EPR spectra should be simulated to extract reliable and biologically meaningful parameters. It is important to point out the coexistence of lateral domains in biological membranes, which recently became evident as a result of a number of different approaches (*6–9*). Additionally, the lateral diffusion of spin-labeled fatty acids and their derivatives is too slow with respect to the EPR CW time scale to average out the differences between the domains. Consequently, this heterogeneous structure of cell membranes results in superimposed spectra composed of several spectral components of the particular domains. Although translational diffusion is slow with respect to EPR CW, it should be stressed that under physiological conditions the rotational motions of molecules are fast.

Generally, to describe the EPR spectra of spin probes, the stochastic Liouville equation is used (*10, 11*). In a membrane system where molecular rotational motions are fast with respect to the EPR time scale, this approach can be simplified (*2, 12–14*), and the magnetic interaction tensors can be averaged over the stochastic rotational motions of the spin-probe molecules. Subsequently, the spin Hamiltonian with averaged tensor components can be used to calculate lineshapes for the spin-probe molecules in membrane segments with a particular orientation relative to the external magnetic field. The spectra of the randomly oriented cell membrane segments are finally summed to get the inhomogeneously broadened spectra. A very similar approach can be used also to study other biological systems (*15*). In situations where slow molecular rotational motions occur, a more sophisticated method for solving the Liouville equation must be applied, as shown for oriented phospholipid bilayers (*16*). However, in the complex geometry of tissues or cell suspensions measured at physiologically relevant temperatures, we believe that the fast-motion approximation satisfactorily describes the EPR spectra and that reliable data can be obtained by the application of optimization methods. Therefore, based on maximum acceptable numerical costs in simulations of nitroxide spectra, we decided to calculate lineshapes based on a model which provides data about ordering, dynamics, and polarity at different locations in the membrane. We believe that this approach allows a sufficiently reasonable description of the spectra of fatty acid spin probes (or their methyl esters) in fluid biological membranes at physiological temperatures. The time consumption allows the ap-

[1] To whom correspondence should be addressed. E-mail: janez.strancar@ijs.si.

1090-7807/00 $35.00

plication of simulation and automatic optimization via procedures to be performed on a Pentium-processor-based personal computer. In this way, the automatic parameter optimization of a series of measurements makes comparison between different samples more objective and enables one to track and detect small but important changes in biological systems.

The goal of this study is to connect the well-established model for the motional-restricted fast-motion approximation (*13*) with experimental and theoretical facts about the lateral membrane heterogeneity and the rigorous optimization routines with statistical validation of the extracted parameters (*16*). We will also discuss the lower sensitivity in characterization of spectra constructed of a broad spectral component by least squares from the point of view of the optimization process. Finally, regarding the optimization routine, we will compare the two procedures (Simplex and Monte Carlo) which do not need the calculation of the derivatives of the least squares function over each spectral parameter. In such cases, the mentioned optimization routines are preferred. However, the derivatives can be obtained numerically if they are required (e.g., the Levenberg–Marquardt algorithm) (*16*).

It should be stressed that the experimental conditions should impose the incorporation of hydrophobic SP into membranes at small local molar concentrations in order to study the membrane domains primarily. However, experiments have been performed where these conditions are not met: for example, using a high concentration of SP, or SP with a low membrane–water partition coefficient, or using additional paramagnetic ion complexes. In these situations, it is necessary to apply the procedure for the treatment of additional spectral components, which are not membrane spectra. These spectral components are characterized by the exchange frequencies, which describe the spin–exchange interaction between paramagnetic molecules (*17, 18*). Two examples of spin–exchange broadened spectra can be simulated by our approach. The first includes the spin–exchange interaction between spin-probe molecules, which is important especially when spin probes form aggregates in the aqueous solution or when the overloading of the membrane with SP is obtained. The overloading of heterogeneous biological samples can be a useful method for studying the asymmetric properties of membranes (*19*). In such cases, the spectral component broadened by the SP–SP spin exchange must be superimposed on the membrane spectra. The second example, which is important in experimental approaches to gain additional information about the system, is the application of paramagnetic broadening agents (Ni^{2+}, Fe^{3+}, Cr^{3+}, etc.), which are used to distinguish between the contributions of different compartments in the cell suspension to the total EPR spectrum (*20*). The spectral component, which is broadened due to the paramagnetic agent–SP spin exchange should be considered.

To gain a reliable characterization of the membrane spectral components and their parameters, we provide an improved least-squares criterion based on a weighted sum scheme. We thoroughly examine the application of two multidimensional optimization algorithms—Simplex and Monte Carlo—with respect to the noise amplitude of the EPR spectra, the number of parameters, and numerical correlations typical for broad EPR spectra of biological samples.

SPECTRAL SIMULATION

Calculation of the EPR Spectral Lineshape

When lipophilic spin probes (SP) are introduced into a cell suspension or tissue, there are several different compartments where SP could be located: solution, membrane domains, outer and inner layer of membranes, aggregates in membranes and in solution, etc. Therefore, the EPR spectrum is a superimposition of several spectral components corresponding to different local environments or domains, differing in their fluidity characteristics due to different lipid–lipid, lipid–protein, and lipid–carbohydrate interactions. To trace the domains experimentally, temperature variation is usually applied as well as multifrequency EPR.

The procedure for spectral calculation can be divided into three parts:

First, the distribution of paramagnetic centers over the resonant field is calculated numerically for each spectral component. The distribution originates from the random distribution of the orientations of the particular membrane segments. Here, an axially symmetric distribution of membrane normal vectors around the external magnetic field axis is assumed. Due to rapid restricted motion in the lipid phase, the resultant effective values of the interaction tensors of the spin Hamiltonian can be described with the order parameter S (*13*). In the experimental frame, these effective values ($g_{\parallel}^{\mathrm{eff}}$, $g_{\perp}^{\mathrm{eff}}$, $A_{\parallel}^{\mathrm{eff}}$, $A_{\perp}^{\mathrm{eff}}$) are still dependent on the angle Θ between the magnetic field direction and the local membrane normal vector, which approximately coincides with the motional-averaged direction of the SP molecule. The angular distribution of the membrane normal vectors $dP(\Theta)/d\Theta$ relative to the external magnetic field as well as the resonant field dependence $B_r(\Theta)$ on the angle Θ should be taken into account in order to calculate the appropriate powderlike resonant field distribution $dP_M(B_r)/dB_r$ for the three hyperfine components of the spectra ($M = 1, 0, -1$), typical for nitroxides:

$$\frac{dP_M(B_r)}{dB_r} = \int_0^{\pi} \frac{dP(\Theta)/d\Theta}{dB_r(\Theta)/d\Theta} \sin(\Theta) d\Theta, \qquad [1]$$

$$B_r(\Theta) = \frac{\hbar\omega - MA^{\mathrm{eff}}(\Theta)}{\mu_B g^{\mathrm{eff}}(\Theta)}. \qquad [2]$$

The resonant field distribution has a resolution of typically 1024 points per sweep width and is calculated from the SP angular (directional) distribution within an ensemble of 2000–

5000 spins. The assumed axial symmetry of the angular distribution $dP(\Theta)/d\Theta$ appears in fibers or in the case of cellular aggregation and precipitation. It also includes spherical symmetry for any randomly directed spherical and nonspherical particles, as in suspensions. The resonant field distribution defined by Eqs. [1] and [2] has one singularity for each value of M. They originate in the zero derivatives $dB_r/d\Theta$ when the normal vector is perpendicular to the magnetic field ($\Theta = \pi/2$) and the weighting sine is equal to 1. As a consequence, the problem can appear in the numerical derivation of a convolution integral which should be calculated in the final step. We solve this problem in the sense of the Stieltjes integral (*21*) with proper normalization. Close to the singular points, we use series expansion, which is accurate enough.

It should be stressed that both magnetic tensors (**g** and **A**) change with the environment of SP molecules (*13, 22*), since the neighboring electric fields influence the electron density distribution. For the spin-probe Tempo in various solvents, the hyperfine constant changes by 0.25 mT whereas the g constant changes from 2.0061 to 2.0056, which is equivalent to a resonant field change of 0.08 mT. Therefore, the changes in both constants are in the same range. Even across the membrane the polarity varies, as was shown for the doxyl group attached to different positions on the acyl chains (*22*). The latter indicates that the polarity correction factor should be fitted for each domain since the average spin-probe position in the membrane can depend on individual domain characteristics. Numerically, it is difficult to calculate accurate corrections of both tensors for small radicals even in a vacuum (*23, 24*). Therefore, the polarity effects are taken into account empirically in the simplest possible way. We use a linear correction factor (polarity correction factor p_g and p_A) which acts on the trace of tensors and characterizes the polarity of the individual components.

The second part of the EPR spectral lineshape calculation is to calculate the relaxation times T_2 or the linewidths $1/T_2$ for the fast-motional regime, which has been proved convenient for small molecules such as lipophilic SP like spin-labeled fatty acids or their esters (*13*). The linewidths for spin probes in oriented systems such as liquid crystal systems can be calculated by considering the anisotropic rotational relaxation times (*2*). According to our experience with membrane spectra composed of several spectral components, the influence of the anisotropic rotational relaxation on the fit becomes small (*25*). This enables us to describe the rotational dynamics within a particular domain with one effective empirical correlation time τ_c. We therefore calculate the Lorentzian linewidths from (*26*) in order to characterize the relative amplitudes of the hyperfine components,

$$\frac{1}{T_2} = A(\tau_c, \mathbf{A}, \mathbf{g}) + B(\tau_c, \mathbf{A}, \mathbf{g})\,M + C(\tau_c, \mathbf{A}, \mathbf{g})\,M^2 + W, \qquad [3]$$

where M represents the nuclear spin projection number ($M = -1$, 0, or 1 for nitrogen) and W represents additional broadening due to unresolved hydrogen superhyperfine structure, the presence of any minor paramagnetic impurities, external field nonhomogeneities, modulation effects, etc. The coefficients A, B, and C are derived using a motional narrowing approximation valid for correlation times in the range $10^{-11} < \tau_c < 10^{-8}$ s (*26*).

A large broadening effect due to spin exchange from spin-probe aggregates is treated differently. In this case, the lineshape is no longer Lorentzian but is calculated from exchange-coupled Bloch equations (*17, 18*). As in other rotational problems, the complex magnetization $\mathcal{g} = \mathcal{M}_x + i\mathcal{M}_y$ is introduced. Considering a typical EPR CW experiment with slow sweep, we can assume that relaxation maintains constant magnetization in the rotating coordinate frame. The effect of the exchange interaction between spins can be incorporated into the steady-state Bloch equations by introducing a term which changes the M_1th spin state of the examined multiplet "1" interacting with the M_2th state of the other multiplet "2",

$$\left(\frac{1}{T_2(M_1)} + i(B - B_{M_1})\right)\mathcal{g}_{M_1} - \sum_{M_1 \neq M_2} W_{M_1M_2}(\mathcal{g}_{M_2} - \mathcal{g}_{M_1}) = -iB_1\mathcal{M}_0, \qquad [4]$$

where B_{M_i} are the resonant fields of the M_ith resonant lines, $W_{M_1M_2} = W^{\text{exc}}$ are the exchange coupling constants (in our model they are approximated to be independent of M_1 and M_2), B_1 is the microwave magnetic field amplitude, and $\mathcal{M}_0$ is the equilibrium magnetization. The system of equations is solved numerically for the imaginary part of the complex magnetization (absorption mode).

The third part of the EPR spectral calculation includes convolution of the resonant field distribution with the Lorentzian absorption line $I(B - B_r; T_2(M))$ for all three lines in the spectra (for $M = 1, 0, -1$):

$$I(B) = \sum_M \left[\int I(B - B_r; T_2(M))\,\frac{dP_M(B_r)}{dB_r}\,dB_r\right]. \qquad [5]$$

Since this convolution includes on the order of only 100 points, the method of calculation is not so important in the sense of the elapsed processing time. Either an FFT-based calculation or direct sums can be used.

Improved Least-Squares Criterion as a Measure of Goodness of Fit

For optimization of the spectral parameters based on comparison between experimental and simulated spectra, one has to decide about the function describing the goodness of fit. In many studies, this function was chosen to be the χ^2 function,

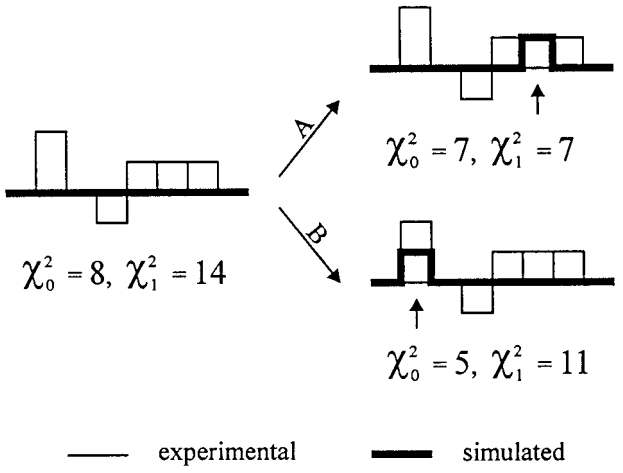

FIG. 1. Demonstration of the sensitivity of the 1-type χ^2 function compared with the 0-type χ^2 function; the thin and the thick lines represent small segments of the experimental and the simulated spectra, respectively; one point (labeled with an arrow) is changed from the left to the right picture.

which is basically the sum of the squared residuals between experimental and model spectra weighted by the standard deviation of the experimental points. After optimization of our fitting procedure, we realized that the χ^2 function is a good criterion for optimizing spectra with sharp lines, typical for solutions, but it seems to be less sensitive for broader spectra typical of spin-labeled membranes. Therefore we introduced an improved χ^2 function (Eq. [6]), where the residuals are summed in "islands" (in further text, the quotation marks will be omitted), spanned between the two neighboring crossings of the experimental and simulated spectra, weighted by a power β of the individual island lengths λ_{island}. The 0-type ($\beta = 0$) is equivalent to the standard χ^2. Finally, the sum over all islands is performed and weighted with the number of all the points N in the whole spectrum, in order to decrease the numbers in numerical calculations:

$$\chi^2_{(\beta)} = \frac{1}{N} \sum_{\text{island}} \left((\lambda_{\text{island}})^{\beta} \sum_{i=1}^{\lambda_{\text{island}}} \frac{(y_{\text{exp}} - y_{\text{sim}})^2}{\sigma^2} \right). \qquad [6]$$

The standard deviation σ is accessed numerically from the experimental points of those parts where simulated spectral derivatives are close to zero (usually at both ends of the spectrum). It is very tedious to demonstrate the difference between the 0- and 1-type of χ^2 on the spectrum with 1024 points. Therefore we will present the benefits of the improved χ^2 on a small segment of a spectrum. What we would like to show is the change in χ^2 if a small perturbation of the spectra is introduced. We compare the sensitivity of the two types of χ^2 function to changes in simulated spectra (Fig. 1). It can be seen that the 1-type χ^2 is more sensitive in detecting broader peaks (change A in Fig. 1), whereas the 0-type χ^2 is relatively more sensitive to narrow peaks (change B in Fig. 1). Therefore we assume that the 1-type χ^2 is a better choice to optimize the parameters describing the membrane spectra.

Optimization of EPR Spectral Parameters

In simulations of the EPR spectra of nitroxide spin probes incorporated into the lipid bilayers of biological membranes in a sample of a cell suspension or tissue, the main problem is the large number of parameters which should be fitted. Due to membrane heterogeneity, the spectrum is a superposition of spectra from several domains which are characterized by different sets of parameters. These are order parameter S, rotational correlation time τ_c, correction factors p_g and p_A for magnetic tensors **g** and **A** due to the polarity of the nitroxide environment, additional broadening W, and the fraction of the individual domain d. To obtain the optimal parameters which characterize the individual domain, we use a multidimensional optimization routine based on the minimization of the improved χ^2 function with island-length weighting. In our optimization routine, we deal with linear Simplex and nonlinear Monte Carlo algorithms.

Simplex algorithm. The Simplex is one of the deterministic methods (gradient, Powell, Levenberg–Marquardt, etc.), which all have approximately the same computational costs relative to slower stochastic methods (Monte Carlo, genetic algorithm). On the other hand, they all have the same disadvantage of convergence to the local minimum of χ^2 instead of to the global minimum, which is not the case with stochastic methods (*27, 28*). The methods which use the derivatives are somewhat more effective but a bit slower. In general, the effect of the optimization routine strongly depends on the phase space characteristics, so the appropriateness of the method cannot be predicted. We chose the Simplex (amoeba) algorithm due to its simplicity, robustness, and the lack of a need for any partial derivatives of χ^2 over any optimizing parameter (*27, 29*).

The optimization routine was explored by applying it to a known synthetic spectrum at different starting parameters and amplitudes of noise. To present the noise effect, we sketch the minima on a two-dimensional cross section of χ^2 over the plane of two parameters p_1 and p_2 (Fig. 2). The construction of the surfaces in Fig. 2 is based on many calculations of χ^2 cross sections (some of them are discussed further under Results and Discussion) and Simplex-based optimizations. It can be seen that low noise sharpens the minima (Fig. 2A). In contrast, high noise broadens the minima (Fig. 2B); consequently smaller local minima almost disappear. As such, the number of minima is reduced and the possibility of finding the global and not the local minima increases. As a result, fitting the spectra with low noise (high signal-to-noise ratio) requires better starting conditions than fitting the spectra with a higher noise level (lower signal-to-noise ratio). It is also obvious that too high noise levels could prevent the extraction of the parameters with the required accuracy. Finally, it is strongly recommended that the

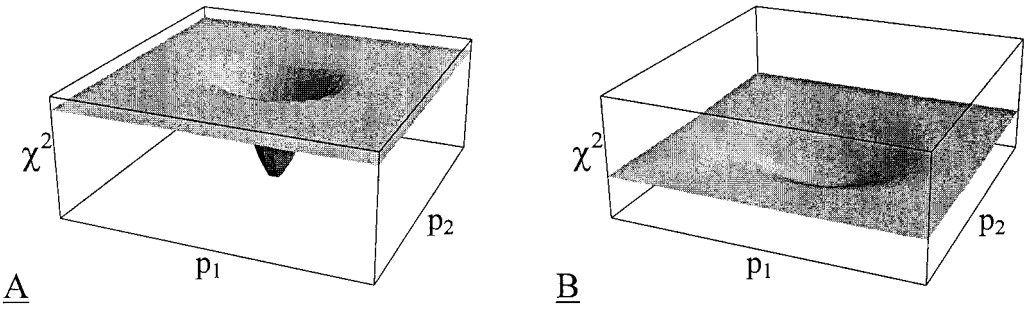

FIG. 2. Schematic presentation of a two-dimensional cross section of χ^2 over the plane of two parameters p_1 and p_2; the demonstration of the suspected noise effect on the shape of the minima in the χ^2 function: (A) lower noise amplitude of 5%; (B) higher noise amplitude of 10%.

optimization be restarted with completely different starting conditions to see if two distant minima exist.

We programmed the Simplex algorithm in a common way constructed from four linear transformations of $n + 1$ sets of parameters, where n is the number of parameters (*27*). The transformations of sets are repeated until χ^2 for the best set does not change significantly between two transformations.

Monte Carlo algorithm. The second algorithm we used is the nonlinear stochastic Monte Carlo procedure. The algorithm is known from thermodynamic and quantum simulations. The basic idea is to change an arbitrary parameter (state) and accept the change according to the Boltzmann probability law, which allows getting out of the local minima with some final probability. With an appropriate response function (cooling when lowering the energy of the state), it is possible to achieve the global minimum.

The standard Monte Carlo scheme consists of three tasks in each step (*27*). First, an arbitrary parameter must be chosen. The parameter is then arbitrarily changed and a new χ^2 calculated. Then the decision to accept the correction proceeds in the

TABLE 1
Comparison between the Convergence of Fitted Spectrum to Spectrum A (Fluid Ordered) and to Spectrum B (Fluid Disordered) after Two Restarts

	S^a	$\tau_c{}^b$ (ns)	W^c (G)	$p_A{}^d$	$p_g{}^e$	Average relative error ^{f}
			Spectrum A			
Original set	0.60	0.60	1.60	1.000	1.000000	0
Starting set	0.45	0.80	1.20	0.950	0.999900	0.22
Optimized set (0-type χ^2, noise 5%)	0.61	0.43	1.73	1.004	1.000004	0.04
Optimized set (1-type χ^2, noise 5%)	0.60	0.64	1.54	0.996	0.999996	0.02
Optimized set (0-type χ^2, noise 10%)	0.56	0.89	1.49	0.971	1.000034	0.13
Optimized set (1-type χ^2, noise 10%)	0.60	0.76	1.47	1.012	0.999985	0.06
			Spectrum B			
Original set	0.30	0.50	1.10	1.050	1.000000	0
Starting set	0.40	0.70	0.80	0.980	1.000100	0.27
Optimized set (0-type χ^2, noise 5%)	0.29	0.52	0.96	1.049	0.999991	0.04
Optimized set (1-type χ^2, noise 5%)	0.31	0.70	0.89	1.037	1.000006	0.07
Optimized set (0-type χ^2, noise 10%)	0.32	1.14	0.62	1.055	1.000011	0.15
Optimized set (1-type χ^2, noise 10%)	0.28	0.60	1.01	1.023	1.000089	0.09

Note. Original, starting, and optimized parameters are presented together with the average of the relative errors of all parameters; comparison is made between 0-type and 1-type χ^2 for noise amplitudes of 5 and 10%.

[a] Order parameter.

[b] Rotation correlation time.

[c] Additional broadening.

[d] Polarity correction factor on the trace of hyperfine coupling tensor **A**.

[e] Polarity correction factor on the trace of spin-magnetic field coupling tensor **g**.

[f] Relative errors are calculated relative to the original values of the parameters except for parameter p_g, where 100% error means absolute change of 10^{-4} in the parameter.

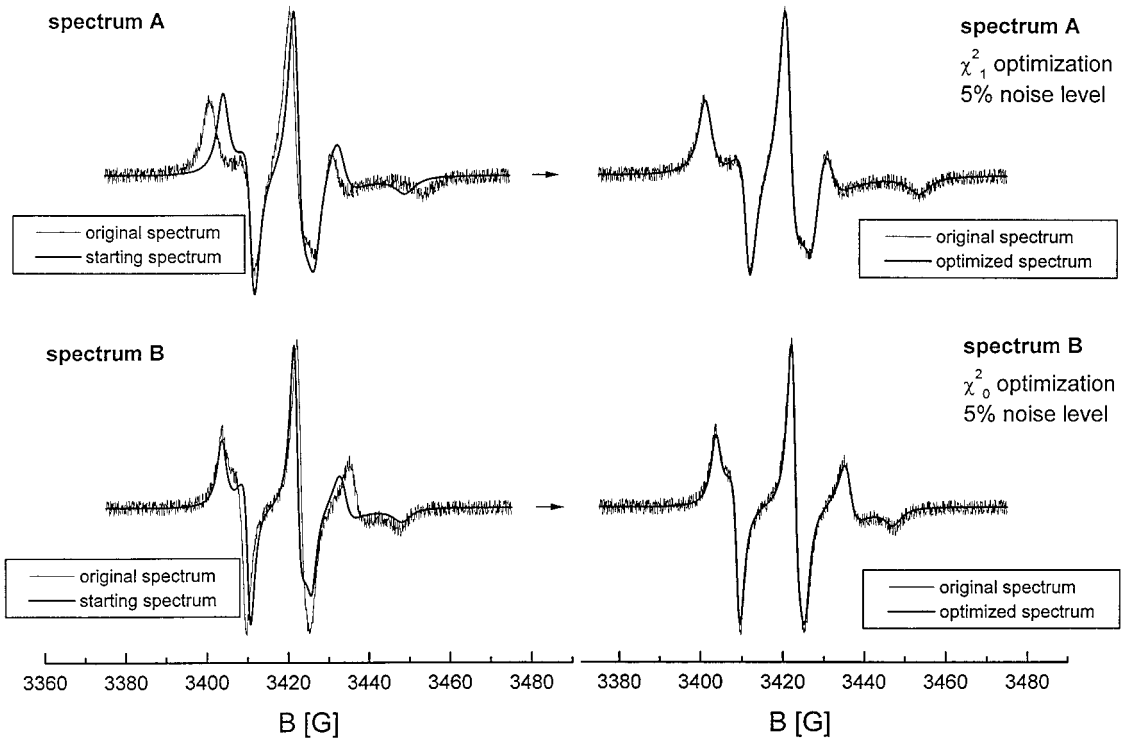

FIG. 3. Optimization of spectra A and B with the starting spectra (starting sets of parameters from Tables 1) on the left and optimized spectra on the right (best fits with 1-type χ^2 and 0-type χ^2 for spectra A and B, respectively).

following way: It is always accepted if the new χ^2 is lower than the previous one. It is also accepted if an arbitrary number between 0 and 1 is lower than the Boltzmann factor $\exp(-\chi^2/T)$ (Metropolis criterion). Finally, if the new correction is accepted, the "temperature" T is corrected according to the cooling function, which is defined by the temperature change in one accepted step,

$$dT = \lambda(\chi^2 - T) - \omega T, \qquad [7]$$

where λ describes the "heat" transfer from the environment to the "system" or vice versa in a single step and ω represents the rate of (slow) cooling of the system independent of the energy (χ^2). If the temperature of the system were too low, the probability of getting out of a minimum would also be too low. This could happen if the system cooled down too fast (too high ω). On the other hand, for too slow cooling, the convergence of the algorithm would take too long (ω approaches 0). So the compromise is accepted when the values of approximately 0.1 for λ and 0.003 for ω were used.

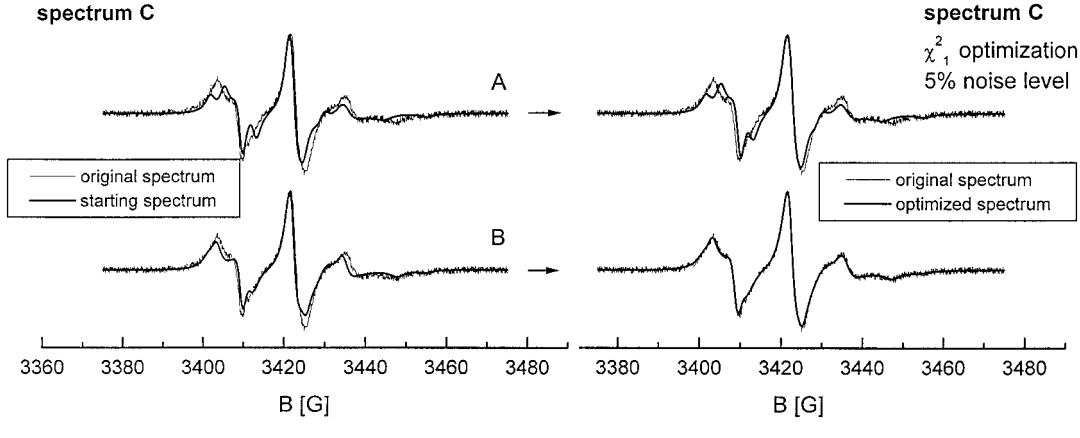

FIG. 4. Optimization of spectrum C with the two starting spectra (A and B with starting sets of parameters 2 and 3 from Table 2, respectively) on the left and optimized spectra on the right (best fits with 1-type χ^2).

TABLE 2
Original and Different Starting Parameter Sets for the Two-Membrane-Domain Spectrum C and the Corresponding Averaged Relative Errors

	Domain 1						Domain 2					
Spectrum C[a]	S	τ_c (ns)	W (G)	p_A	p_g	d_1	S	τ_c (ns)	W (G)	p_A	p_g	Average relative error[b]
Original set	0.60	0.60	1.60	1.00	1.00000	0.40	0.30	0.50	1.10	1.05	1.00000	0
Starting set 1	0.45	0.80	1.20	0.95	0.99990	0.55	0.40	0.70	0.80	0.98	1.00010	0.26
Starting set 2	0.70	0.40	1.20	0.95	0.99990	0.55	0.25	0.70	0.80	0.98	1.00010	0.23
Starting set 3	0.64	0.50	1.40	0.98	0.99995	0.48	0.34	0.40	1.00	1.03	1.00005	0.11

[a] For description of the parameters, see Table 1.
[b] Relative errors are calculated relative to the original values of the parameters except for parameter p_g, where 100% error means an absolute change of 10^{-4} in the parameter.

We know that in our optimization procedures some parameters are less sensitive than others. Therefore, to reduce the number of steps, we add a "sensitivity table" in which the probabilities of choosing an arbitrary parameter during the MC steps are presented. The sensitivity table is calculated at the beginning of the algorithm and recalculated every time any correction is accepted. The probability $P(a_i)$ of each parameter a_i is estimated from the alteration of χ^2, when the particular parameter a_i is changed, divided by the amplitude of this (parameter) change Δa_i, and finally normalized to the sum of all probabilities of choosing the arbitrary parameter:

$$P(a_i) = \frac{\Delta\chi^2(a_i)/\Delta a_i}{\sum_i(\Delta\chi^2(a_i)/\Delta a_i)},$$
$$\Delta\chi^2(a_i) = \chi^2(a_i + \Delta a_i) - \chi^2(a_i). \qquad [8]$$

RESULTS AND DISCUSSION

Optimization of Simulated Spectra with the Simplex Algorithm

Synthetic spectra. The best way to study the sensitivity of the optimization routines is to fit a spectrum with known parameters (simulated spectrum). Only in such a case can complete agreement between calculated and fitted spectra be achieved (no systematic errors). In this study, we wanted to compare the sensitivity of the Simplex procedure based on minimization of two different types of χ^2 function and to test the accuracy of convergence with respect to the signal-to-noise ratio. In our discussion, "convergence" means the decrease of the differences between fitted and known parameters.

We introduce three different types of synthetic spectra with

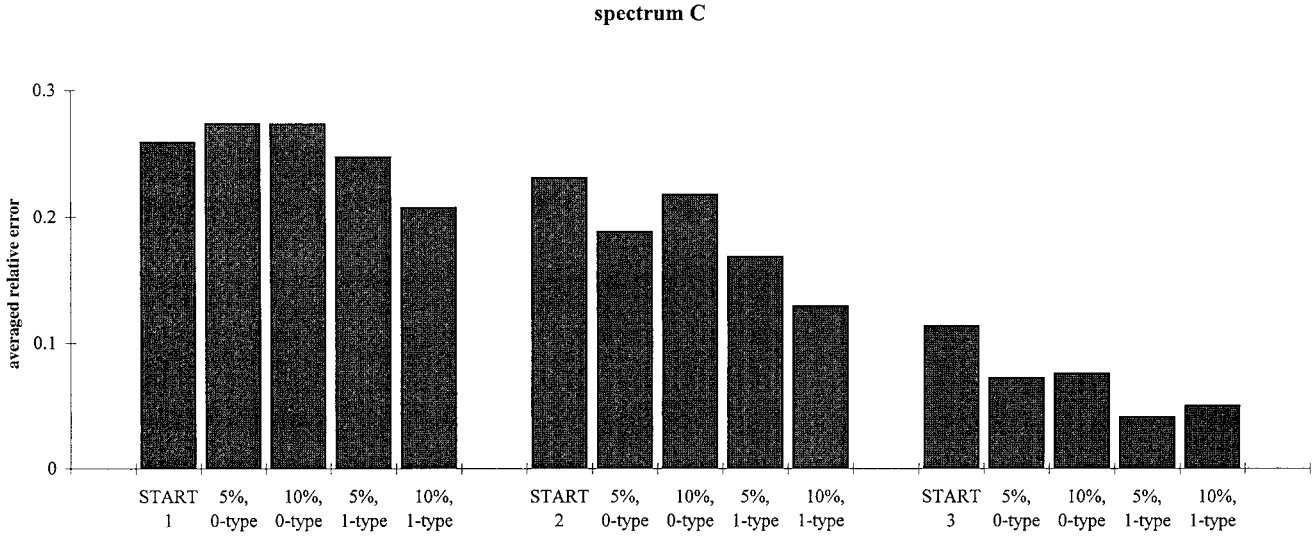

FIG. 5. Comparison between averaged relative errors after optimization of fits with spectrum C at different starting conditions with one restart; comparison between 0-type and 1-type χ^2 for noise amplitudes of 5 and 10%.

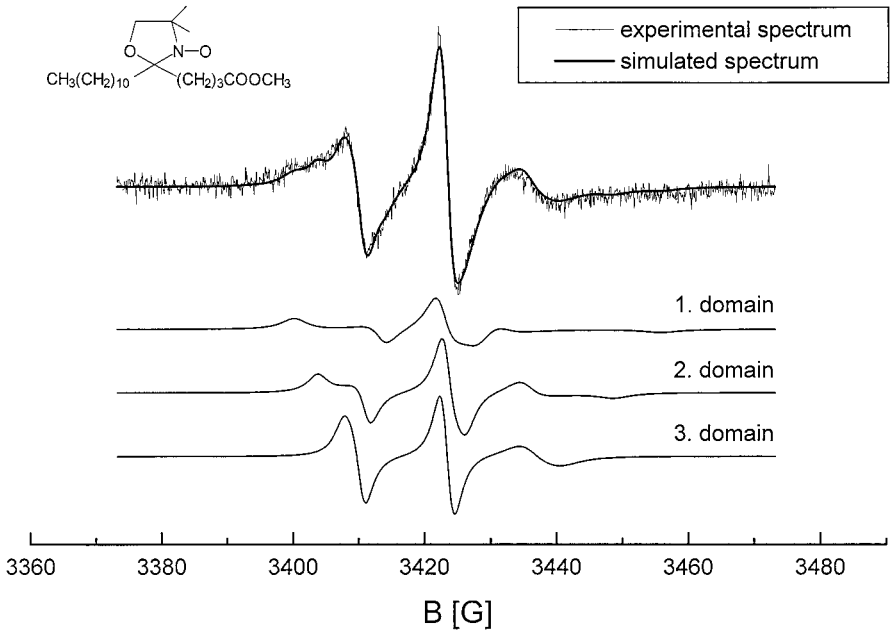

FIG. 6. EPR spectrum of the spin-labeled methyl ester of 5-doxylpalmitate (MeFASL(10,3)) in the membrane of human leukocytes. The suspension of undamaged leukocytes was spin-labeled by the MeFASL(10,3). One milliliter of cell suspension (10^7 cell/ml) was incubated for 15 min at room temperature with 10 nmol of spin probe, which was prepared as a thin film on the walls of the glass tube. The suspension was centrifuged at 300*g*, the pellet was put in a glass capillary, and the spectrum was measured on an ESP 300 Bruker EPR CW spectrometer at room temperature. The thin and the thick lines represent experimental and 1-type χ^2 optimized spectra with three spectral components (domains), respectively, with the parameters presented in Table 3. The structural formula of MeFASL(10,3) is also presented.

known parameters. The first two are one-domain spectra representing fluid-ordered membrane vesicles (spectrum A) and fluid-disordered membrane vesicles (spectrum B). The third, two-domain spectrum (spectrum C), a superimposition of spectra A and B, resembles a realistic membrane spectrum.

First, we checked the convergence of the optimization using spectrum A at different noise amplitudes. The starting parameter set is shown in Table 1. We observed that with low noise amplitudes (up to 1.9%) the optimization fails to converge because the minimum in χ^2 is too sharp (Fig. 2A) and could easily be missed with the Simplex procedure. At high noise levels the convergence is less efficient since noise broadens the shape of the minimum (Fig. 2B). Consequently, there exists an optimal value of noise amplitude where the convergence is most effective. Therefore, in subsequent analyses, we checked the convergence at two different noise amplitudes, 5 and 10%.

In the second stage, we compare the optimization of 0- and 1-type χ^2 functions at 5 and 10% noise amplitudes. In Tables 1 and 2 the sets of parameters of the introductory spectra, starting conditions, and optimized spectra are presented together with the averaged relative errors. The relative errors are calculated as the differences between the optimized and original parameters divided by the original parameters (in the case of p_g, it is divided by 10^{-4} instead of 1 for the sake of sensitivity). On the basis of the results presented in Table 1, we can conclude that it is better to fit and optimize the spectra of fluid-ordered membranes (spectrum A, Fig. 3) with the 1-type χ^2 rather than with the 0-type χ^2 for both noise amplitudes. For the spectra of more fluid-disordered membranes (spectrum B, Fig. 3), the optimization based on 0-type χ^2 is better than the optimization with 1-type χ^2 only at 5% noise.

The optimization procedure for a more complex spectrum (spectrum C, Fig. 4) was tested for reproducibility of the Simplex algorithm procedure with different starting conditions (Table 2). It can be seen from Figs. 4 and 5 and Table 2 that to

TABLE 3

Fitted Parameters of the EPR Spectrum of MeFASL(10,3) in the Membranes of Human Leukocytes (See Fig. 6 Legend) with the Standard Deviations Calculated from the Covariance Matrix

Parameter[a]	Domain 1	Domain 2	Domain 3
S	0.68 ± 0.05	0.37 ± 0.03	0.15 ± 0.02
τ_c[b] (ns)	0.8 ± 0.6	0.9 ± 0.5	1.6 ± 0.5
W[b] (G)	1.6 ± 0.6	0.9 ± 0.5	0.5 ± 0.3
p_A	1.00 ± 0.02	1.02 ± 0.01	0.92 ± 0.01
p_g	0.99985 ± 0.00005	0.99988 ± 0.00002	1.00013 ± 0.00003
d	0.38 ± 0.08	0.34 ± 0.9	0.28 ± 0.03

[a] For description of the parameters, see Table 1.

[b] Rotational correlation times and additional broadening of the same domain are usually highly anticorrelated with a correlation coefficient between −90 and −65% (determined from covariance matrix analysis).

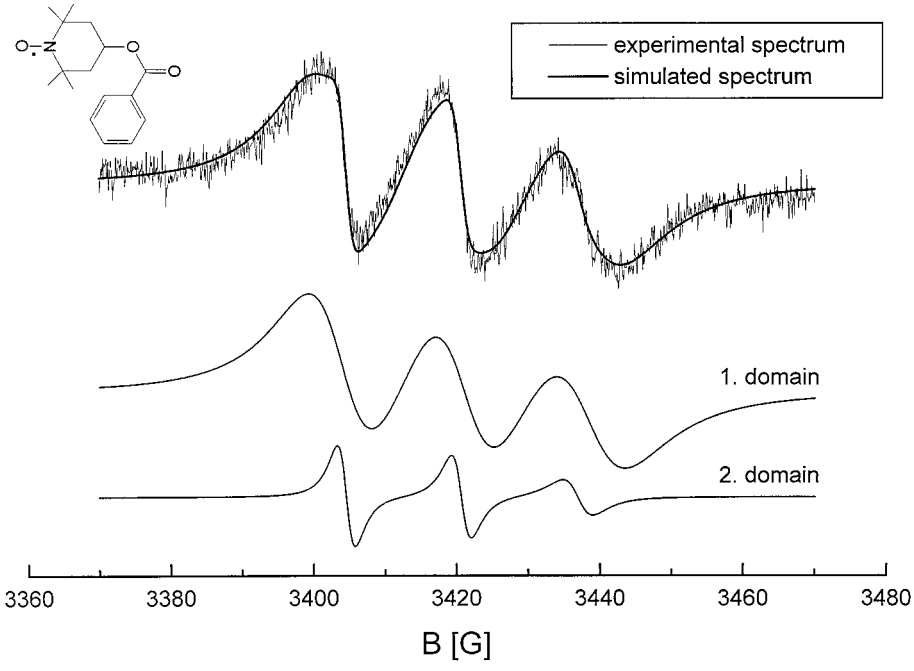

FIG. 7. EPR spectrum of Tempyl benzoate (TBZ) in the membrane of the liposomes made from dipalmitoylphospatidylcholine and cholesterol with the mass ratio of 2:1 in phosphate buffer saline. The liposome suspension was prepared by the thin-film method. One hundred microliters of liposome suspension containing 4.8 mg of lipids was incubated for 15 min at room temperature with 10 nmol of spin probe, which was prepared as a thin film on the walls of the glass tube. The labeled suspension was mixed with 60 mM $K_3(Cr(C_2O_4)_3)$ and put in a glass capillary, and the spectrum was measured on an ESP 300 Bruker EPR CW spectrometer at room temperature. The thin and the thick lines represent experimental and 1-type χ^2 optimized spectra with two spectral components (domains), respectively, with the parameters presented in Table 4. The structural formula of TBZ is also presented.

get a good fit for multidomain spectra the starting approximation should not deviate much more than 20% from the original values (on average). Again, better agreement with the original spectrum was achieved with the optimization procedure based on the 1-type χ^2 than with that based on the 0-type χ^2.

Real membrane spectra. To test the 1-type χ^2-based Simplex optimization on complex experimental spectra, two examples are presented:

1. The EPR spectrum of the methyl ester of 5-doxylpalmitic acid in human leukocyte membranes is presented in Fig. 6 together with the structural formula of the spin probe and the best fit. A good fit is obtained if the spectrum is fitted as a superposition of three spectra by successive optimizations with the Simplex algorithm. The parameters of all the spectral components, as well as the standard deviations that are calculated from the covariance matrix diagonal elements, are presented in Table 3.

2. The dipalmitoylphosphatidylcholine–cholesterol liposomes were labeled with Tempylbenzoate. The broadening agent chromium oxalate ($K_3(Cr(C_2O_4)_3)$) was added into the aqueous phase. In Fig. 7 the EPR spectrum and the corresponding fit obtained by the successive optimizations are presented together with the structural formula of the spin probe. For the spin probe used, it is typical that its nitroxide group almost freely tumbles above the membrane surface. Consequently, when the chromium oxalate is present in the water compartment of the liposome suspension, strong spin-exchange occurs between the nitroxide group and the chromium complex and a typical spin-exchange-broadened spectrum appears. A good fit was obtained by the superposition of two spectra corresponding to regions: in one the spin probe is easily accessible to the broadening agent (spin-exchange-broadened component), whereas in the other it is not (pure isotropic component). The optimized parameters and the standard deviations that were calculated from the covariance matrix diagonal elements are presented in Table 4.

TABLE 4

Fitted Parameters of the EPR Spectrum of Tempyl Benzoate in the DPPC–Cholesterol Liposomes in the Presence of the Paramagnetic Broadening Agent (CrOx) (See Fig. 7 Legend) with the Standard Deviations Calculated from the Covariance Matrix

Parameter[a]	Domain 1[b]	Domain 2[b]
τ_c (ns)	0.7 ± 0.1	0.8 ± 0.3
W^{exc} (G)	8.1 ± 0.3	1.6 ± 0.4
p_A	1.11 ± 0.01	1.04 ± 0.04
p_g	0.99990 ± 0.00005	1.00000 ± 0.00005
d	0.96 ± 0.01	0.04 ± 0.01

[a] For description of the parameters, see Table 1.

[b] In both domains, the angular distribution of the nitroxide group of the spin probes is isotropic (order parameters $S_{1,2} \rightarrow 0$).

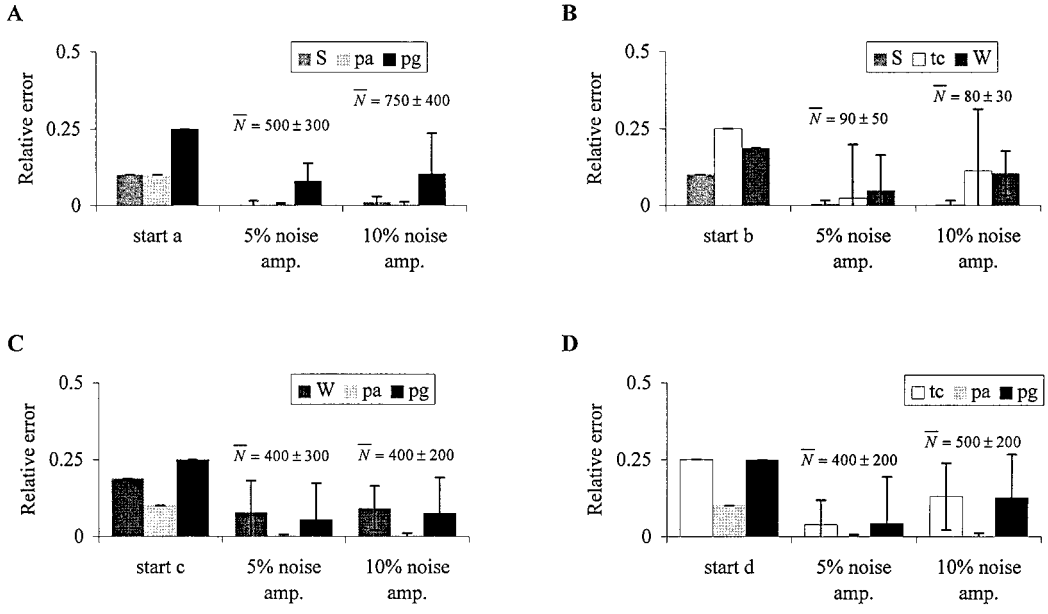

FIG. 8. Averaged relative errors after Monte Carlo optimization of fitted spectrum to spectrum A for different starting conditions and parameter sets for noise amplitudes 5 and 10%. N is the average number of steps in the optimization procedure obtained from 10 individual optimizations. Groups of three parameters were fitted: (A) S–p_A–p_g, (B) S–τ_c–W, (C) W–p_A–p_g, and (D) τ_c–p_A–p_g.

To conclude, the most valuable parameters are the order parameters S_i, weights d_i (i.e., portions of spin probes in a certain domain in the membrane), and polarity corrections $p_{A,i}$ and $p_{g,i}$, as can be seen from Table 3. The linewidth parameters $\tau_{c,i}$ and W_i are highly anticorrelated and therefore less reliable.

Optimization of Simulated Spectra with the Monte Carlo Algorithm

In the second part of our work, the Monte Carlo algorithm for optimization of the parameters of a one-domain spectrum (spectrum A, Fig. 3) was examined at different noise amplitudes and under different starting conditions. The results were compared with those obtained with the Simplex routine based on 1-type χ^2 optimization.

We allow the variation of three parameters for one-domain spectra, with the remaining two parameters being locked to the known values. The two parameters S and p_A by which the position of the lines is influenced generally converge well to their original values whereas with τ_c, W, and p_g the convergence is not so good, as indicated by the large uncertainty bars of the differences between fitted and original parameters (Fig. 8), especially at the higher noise amplitude. To better understand the optimization, four two-parameter cross sections of χ^2 were calculated and presented in Fig. 9. From the cross sections, it can be seen that the S–p_A (Fig. 9C) cross section exhibits a very sharp minimum, which means that the parameters S and p_A are not correlated with respect to the improved least-squared criterion. On the other hand, the τ_c–W, S–τ_c, and S–W cross sections (Figs. 9D, 9B, and 9A, respectively) have broad minima, which indicates numerical correlation between the τ_c and W (also derived by covariance matrix analysis). This could also explain why these two parameters are less sensitive and less accurate.

It should be pointed out that the use of the Monte Carlo optimization routine is not limited to one-domain spectra, which was the case in the above consideration for the sake of simplicity. It is, however, rather limited with respect to the degrees of freedom (number of parameters) and by the presence of high correlations between some parameters. The computing time, which should not exceed some ten minutes for one optimization in order to try different starting conditions, limits the number of parameters to 10 while working with Monte Carlo. In the case of multidomain spectra, spectroscopists should set up the experiment in a way which allows the extraction of the parameters step by step, in small groups of three to six parameters.

CONCLUSIONS

On the basis of the simulation of different types of synthetic spectra under different starting conditions and signal-to-noise ratios, it was shown that better fits are obtained when a new way of characterizing the goodness of fit with "island-length-weighted" χ^2 (1-type χ^2) is used instead of the standard least-squars criterion.

Taking this into account, two examples of real spectra of nitroxide spin probes in membranes were fitted. The EPR spectrum of nitroxide in human leukocytes is fitted well as a

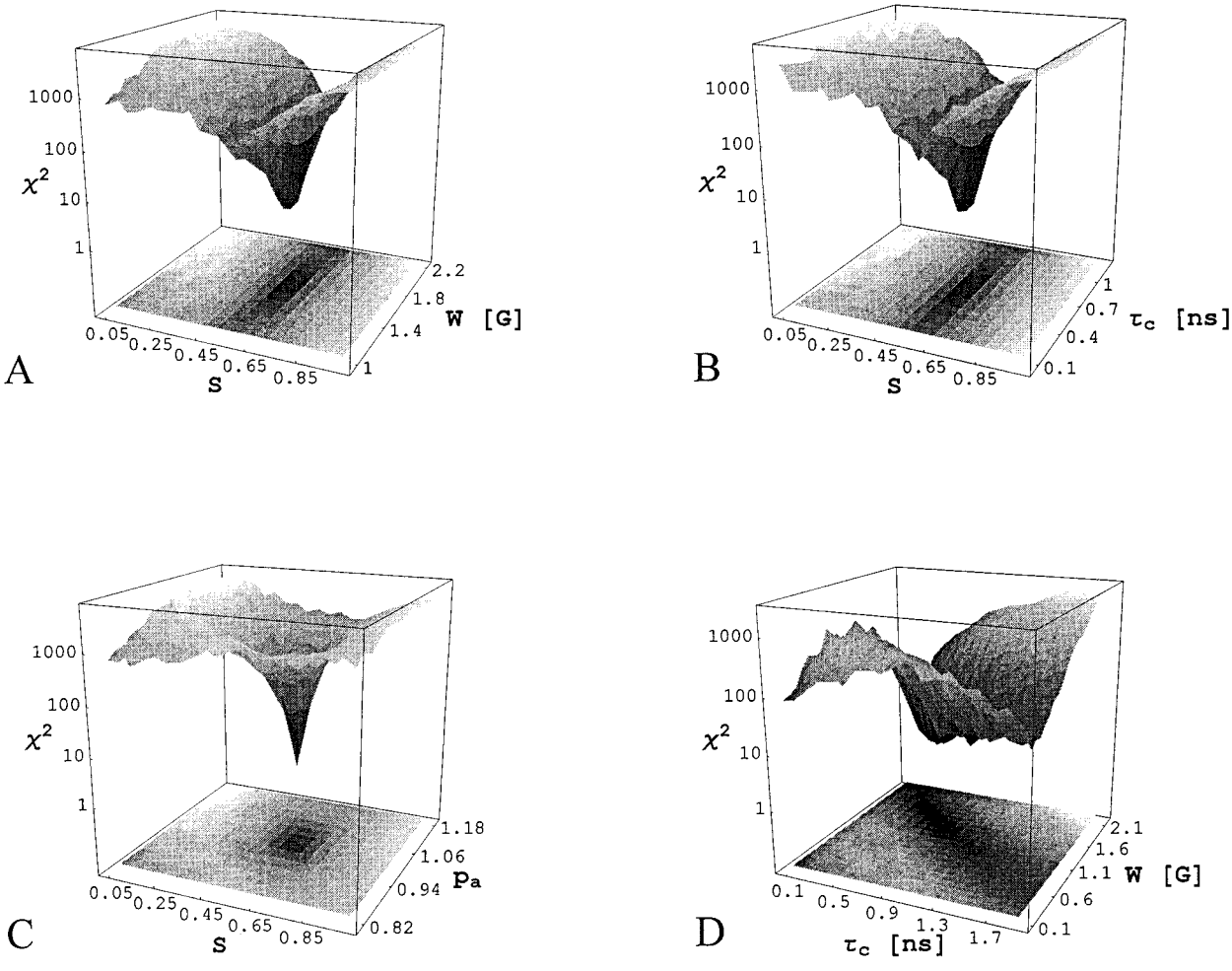

FIG. 9. Four two-parameter cross sections of the 1-type χ^2 function through the phase space: (A) S–W, (B) S–τ_c, (C) S–p_A, (D) τ_c–W; χ^2 of the fits to spectrum A with 5% noise amplitude.

superposition of spectra with different fluidity characteristics. In the other example, where the spectrum of nitroxide in liposome membranes in the presence of paramagnetic broadening agents is presented, the experimental spectrum is well described by the simulation if the spin-exchange interactions between spin probes and paramagnetic ions are taken into account. Comparing the two optimization routines, Simplex and Monte Carlo, we can conclude that the Simplex can be very successful if the starting point is not too far from the original parameters, whereas the Monte Carlo is limited to approximately 10 parameters because of the complexity of the phase space. Both optimization procedures showed problems, with two parameters describing the linewidths (τ_c and W) while other parameters converged very fast (confirmed also by the covariance matrix analysis). Therefore it would be advisable to measure one of the linewidth parameters independently and to approach the optimal combination of fitted parameters by successive optimizations in groups of five to eight parameters with the others fixed.

On the basis of this study, a program for lineshape simulation and optimization was prepared (EPRSIM Version 2.6) (*30*), which is routinely used in our biophysical laboratory. It allows 1024-point EPR spectral simulations with up to five spectral components and optimization of all spectral parameters by two described optimization routines. With this method, it is no longer a problem to resolve two to three membrane domains with different fluidity characteristics in a fast motional regime (10^{-11}–10^{-8} s) in addition to one isotropic component from the solution and the isotropic aggregates located either in the solution or at the membrane surfaces.

ACKNOWLEDGMENT

The work was carried out with the financial support of the Ministry of Science and Technology of Slovenia.

REFERENCES

1. D. Marsh, Electron spin resonance: Spin labels, *in* "Membrane Spectroscopy" (E. Grell, Ed.), pp. 51–142, Springer-Verlag, Berlin (1981).

2. H. Schindler and J. Seelig, EPR spectra of spin labels in lipid bilayers, *J. Chem. Phys.* **59,** 1841–1850 (1973).
3. M. Šentjurc, M. Zorec, M. Čemažar, M. Auersperg, and G. Serša, Effect of vinblastine on cell membrane fluidity in vinblastine-sensitive and -resistant HeLa cells, *Cancer Lett.* **130,** 183–190 (1998).
4. A. A. Cader, D. A. Butterfield, B. A. Watkins, B. H. Chung, and B. Hennig, Electron spin resonance studies of fatty acid-introduced alterations in membrane fluidity in cultured endothelial cells, *Int. J. Biochem. Cell Biol.* **27,** 665–673 (1995).
5. M. Šentjurc, M. Sok, and G. Serša, Plasma membrane fluidity alterations in cancerous tissues, *Radiol. Oncol.* **32,** 109–117 (1998).
6. O. G. Mouritzen and K. Jørgensen, Dynamical order and disorder in lipid bilayers, *Chem. Phys. Lipids* **73,** 3–25 (1994).
7. D. Marsh, Lipid–protein interactions and heterogeneous lipid distribution in membranes, *Mol. Membr. Biol.* **12,** 59–64 (1995).
8. J. Svetek, V. Furtula, M. Nemec, E. A. Nothnagel, and M. Schara, Transport and dynamics dissolved in maize root cortex membranes, *J. Membr. Biol.* **143,** 19–28 (1995).
9. J. Žel, J. Svetek, H. Črne, and M. Schara, Effect of aluminium on membrane fluidity of the mycorrhizal fungus *Amanita muscaria, Physiol. Plant.* **89,** 172–176 (1987).
10. D. J. Schneider and J. H. Freed, Calculating slow motional magnetic resonance spectra, *in* "Biological Magnetic Resonance: Spin Labeling, Theory and Applications" (L. J. Berliner and J. Reuben, Eds.), pp. 1–76, Plenum, New York (1989).
11. B. Robinson, H. Thomann, A. Beth, P. Fayer, and L. R. Dalton, The phenomenon of magnetic resonance: Theoretical consideration, *in* "EPR and Advanced EPR Studies of Biological Systems" (L. R. Dalton, Ed.), pp. 11–110, CRC Press, Boca Raton, FL (1984).
12. S. P. Van, G. B. Birrell, and O. H. Griffith, Rapid anisotropic motion of spin labels: Models for motion averaging of the ESR parameters, *J. Magn. Reson.* **15,** 444–459 (1974).
13. O. H. Griffith and P. C. Jost, Lipid spin labels in biological membranes, *in* "Spin Labeling, Theory and Application" (L. J. Berliner, Ed.), pp. 453–523, Academic Press, New York (1976).
14. W. L. Hubbell and H. M. McConnell, Molecular motion in spin-labeled phospholipids and membranes, *J. Am. Chem. Soc.* **93,** 314–326 (1971).
15. V. Timofeev and B. Samarianov, Dynamics of macromolecule spin-labeled side-chain groups by EPR spectra simulation, *J. Chem. Soc., Perkin Trans. II* **12,** 2175–2182 (1995).
16. D. E. Budil, S. Lee, S. Saxena, and J. H. Freed, Nonlinear-least squares analysis of slow-motion EPR spectra in one and two dimensions using a modified Levenberg–Marquardt algorithm, *J. Magn. Reson. A* **120,** 155–189 (1996).
17. Y. N. Molin, K. M. Salikhov, and K. I. Zamaraev, "Spin Exchange, Principles and Applications in Chemistry and Biology," Chap. 2, pp. 36–41, Springer-Verlag, New York (1980).
18. E. Sackmann and H. Träuble, Studies of the crystalline–liquid phase transition of lipid model membranes, parts 1–3, *J. Am. Chem. Soc.* **94,** 4482–4510 (1972).
19. J. Štrancar, O. Zorko, M. Nemec, J. Svetek, and M. Schara, Domain structure of biological membranes as studied by EPR, *Period. Biol.* **100,** 29–33 (1998).
20. M. Anžur, B. Tome, M. Šentjurc, and M. Schara, Cellular volume determination of fungus *Claviceps purpurea* Schrotic cells. *Biotechnol. Bioeng.* **28,** 1879–1883 (1986).
21. G. A. Korn and T. M. Korn, "Mathematical Handbook for Scientists and Engineers," Chap. 4, pp. 112–114, McGraw-Hill, New York (1961).
22. O. H. Griffith, P. J. Dehlinger, and S. P. Van, Shape of hydrophobic barrier of phospholipid bilayers. Evidence for water penetration in biological membranes, *J. Membr. Biol.* **15,** 159–192 (1974).
23. D. Yayatilaka, Electron spin resonance **g** tensors from general Hartree–Fock calculations, *J. Chem. Phys.* **108,** 7587–7594 (1998).
24. G. Schreckenbach and T. Ziegler, Calculation of the **g**-tensor of electron paramagnetic resonance spectroscopy using gauge-including atomic orbitals and density functional theory, *J. Phys. Chem.* **101,** 3388–3399 (1997).
25. M. Žuvič-Butorac, P. Müller, T. Pomorski, J. Libera, A, Hermann, and M. Schara, Lipid domains in the exoplasmic and cytoplasmic leaflet of the human erythrocyte membrane: A spin label approach, *Eur. Biophys. J.* **28,** 302–311 (1999).
26. P. L. Nordio, General magnetic resonance theory, *in* "Spin Labeling, Theory and Application" (L. J. Berliner, Ed.), pp. 5–51, Academic Press, New York (1976).
27. W. H. Press, "Numerical Recipes: The Art of Scientific Computing," Chap. 10, pp. 274–334, Cambridge Univ. Press, Cambridge, UK (1989).
28. W. H. Press, "Numerical Recipes: The Art of Scientific Computing," Chap. 14, pp. 521–538, Cambridge Univ. Press, Cambridge, UK (1989).
29. P. G. Fayer, R. L. H. Bennett, C. F. Polnaszek, E. A. Fayer, and D. D. Thomas, General method for multiparameter fitting of high-resolution EPR spectra using a Simplex algorithm, *J. Magn. Reson.* **88,** 11–125 (1990).
30. J. Štrancar, EPRSIM version 2.6 for Windows NT, available via Internet page http://www2.ijs.si/~jstrancar/ (1999).